

Studies of Solution Character by Molecular Spectroscopy.

VI. Experimental Methods in Ion Site Characterization.

Solvents with Simple Site Character

Walter F. Edgell* and Angelo Barbetta

Contribution from the Department of Chemistry, Purdue University,
West Lafayette, Indiana 47907. Received April 23, 1973

Abstract: A study of the ion sites present when $\text{NaCo}(\text{CO})_4$ is dissolved in a variety of solvents is begun. The method used is a computer-aided analysis of the infrared band arising from the F_2CO stretching modes of the anion near 1900 cm^{-1} . The improved experimental methods required by both the nature of the problem and the accuracy of the analysis are presented. These involve sample preparation and handling as well as the procedures for obtaining spectra. The methods are applied to solutions of the salt in dimethyl sulfoxide, dimethylformamide, nitromethane, hexamethylphosphoramide, acetonitrile, and pyridine. While these solutions show what appears to the unaided eye as a single band, the analysis shows that two components are present—a main component with virtually all of the intensity and a very weak side band. The latter is found to arise from the 1.1% of ^{13}C in the $\text{Co}(\text{CO})_4^-$ anion. The ion sites have an effective potential energy of tetrahedral (or higher) symmetry. Only solvent molecules are near-neighbors of an ion in these solutions. The role of the solvent-surrounded ion site in the chemistry of the $\text{Co}(\text{CO})_4^-$ anion is illustrated with an example. The nature of this ion site is considered in terms of some aspects of the ion-solvent interaction, and the physical properties which a solvent must have to generate it are discussed. Some comments are made on the frequency, intensity, and half-widths of the two band components in the six solvents.

The structure of a solution at an ion site is a matter of interest to chemists. It plays a role in understanding the physical properties of electrolytic solutions and can be expected to contribute to the knowledge of reaction paths and the catalysis of reactions taking place in these solutions.

Spectroscopy is a primary tool in obtaining this structural knowledge. Extensive studies of carbanion salts in nonaqueous solvents have been made with electron spin resonance, nuclear magnetic resonance, and ultraviolet spectroscopy by a group of workers far too numerous to cite individually here. We mention Weissman,¹ Szwarc, Hogen-Esch, and Smid,² and de Boer³ and their coworkers and refer the reader to the recent excellent review of the field edited by Szwarc.⁴ Raman spectroscopy, in a series of studies by Plane,⁵ Irish,⁶ and Walrafen,⁷ has provided extensive information about aqueous solutions of salts of the nitrate ion. Information about the nature of the environment of the alkali ion for a variety of salts in nonaqueous solvents has been obtained from a study of the far-infrared band due to the cation motion by Edgell,⁸ Popov,^{9a} Risen,^{9b} and their coworkers.

In the latter studies, it is observed that in certain solvents, e.g., THF, the frequency of the translational¹⁰ motion of the cation changes as the salt anion is changed.⁸ One concludes that the anion must be a near neighbor of the cation in a tight ion-pair or similar structure. In other solvents extensively studied by Popov,^{9a} e.g., DMSO, the cation frequency is independent of the salt anion, and the dominant structures here are loose ion pairs and "free" ions.

Recently, it was shown that an examination of the contour of the infrared (or Raman) bands associated with the internal vibration of the $\text{Co}(\text{CO})_4^-$ anion provides a sensitive probe of ion site structure in nonaqueous solutions.¹¹ In that work, it was possible to detect the presence of two kinds of ion sites in THF and to estimate the population of each site. As a result of these findings, we are carrying out an extensive study of the ion sites for $\text{NaCo}(\text{CO})_4$ in a variety of solvents. Primary goals of the work are to find out

(1) (a) N. M. Atherton and S. I. Weissman, *J. Amer. Chem. Soc.*, **83**, 1330 (1961); (b) P. J. Zanstra and S. I. Weissman, *ibid.*, **84**, 4408 (1962).

(2) (a) T. E. Hogen-Esch and J. Smid, *J. Amer. Chem. Soc.*, **88**, 307 (1966); (b) R. V. Slates and M. Szwarc, *ibid.*, **89**, 6043 (1967); (c) B. Lundgren, S. Claesson, and M. Szwarc, *Trans. Faraday Soc.*, **66**, 3053 (1970).

(3) (a) G. W. Canters and E. de Boer, *Mol. Phys.*, **13**, 395 (1967); (b) G. W. Canters, B. M. P. Hendricks, and E. de Boer, *J. Chem. Phys.*, **53**, 445 (1970).

(4) M. Szwarc, "Ions and Ion-Pairs in Organic Reactions," Wiley-Interscience, New York, N. Y., 1972.

(5) R. E. Hester and R. A. Plane, *J. Chem. Phys.*, **40**, 411 (1967); **45**, 4588 (1966); A. T. Lemley and R. A. Plane, *ibid.*, **57**, 1648 (1972).

(6) A. R. Davis and D. E. Irish, *Inorg. Chem.*, **7**, 1699, 2565 (1968); D. E. Irish, G. Charf, and D. L. Nelson, *ibid.*, **9**, 425 (1970).

(7) (a) R. E. Hester, R. A. Plane, and G. E. Walrafen, *J. Chem. Phys.*, **39**, 249 (1963); (b) G. E. Walrafen, *ibid.*, **43**, 479 (1965); (c) D. E. Irish and G. E. Walrafen, *ibid.*, **46**, 378 (1967).

(8) (a) W. F. Edgell and A. T. Watts, Abstracts, Symposium on Molecular Structure and Spectroscopy, Ohio State University, June 1965,

p 85; (b) W. F. Edgell, A. T. Watts, J. Lyford, IV, and W. Risen, Jr., *J. Amer. Chem. Soc.*, **88**, 1815 (1966); (c) W. F. Edgell, Abstracts, 153rd National Meeting of the American Chemical Society, Miami Beach, Fla., April 1967, No. R-149; (d) W. F. Edgell, J. Lyford, and J. Fisher, Abstracts, 155th National Meeting of the American Chemical Society, San Francisco, Calif., April, 1968, No. S-136; (e) W. F. Edgell, J. Lyford, IV, Rose Wright, W. Risen, Jr., and Alan Watts, *J. Amer. Chem. Soc.*, **92**, 2240 (1970).

(9) (a) B. W. Maxey and A. I. Popov, *J. Amer. Chem. Soc.*, **89**, 2230 (1967); **91**, 20 (1969); J. L. Wuepper and A. I. Popov, *ibid.*, **91**, 4352 (1969); **92**, 1493 (1970); M. K. Wong, W. J. McKinney, and A. I. Popov, *J. Phys. Chem.*, **75**, 56 (1971); W. J. McKinney and A. I. Popov, *ibid.*, **74**, 535 (1970). (b) A. T. Tsatsas and W. Risen, Jr., *J. Amer. Chem. Soc.*, **92**, 1789 (1970); A. T. Tsatsas, R. Stearns, and W. Risen, Jr., *ibid.*, **94**, 5247 (1972).

(10) There is a nomenclature problem here. It has been the practice to refer to the infrared band involved as arising from the intermolecular vibration of the ion, referring to the back and forth character of the motion. However, it is the center of mass of the alkali ion that is changing and one may speak of this motion as the translation of the ion, using such words as "oscillatory" to describe its character. The point is most significant when one deals with a polyatomic ion, e.g., $\text{Co}(\text{CO})_4^-$, which can vibrate as well as translate (and rotate).

(11) (a) W. F. Edgell, J. Lyford, IV, A. Barbetta, and C. I. Jose, *J. Amer. Chem. Soc.*, **93**, 6403 (1971); (b) W. F. Edgell and J. Lyford, IV, *ibid.*, **93**, 6407 (1971).

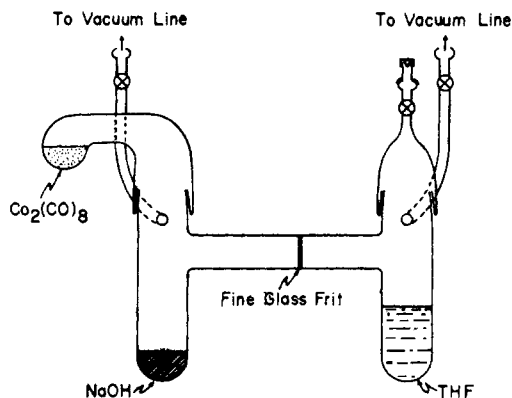


Figure 1. Reaction apparatus.

how many different kinds of ion sites exist, to identify them, and to learn something about the role of the solvent in fixing which ion site or mix of ion sites are present in a given solution. In this paper, we report the experimental and the analytical methods which have been developed for the work and the results for six solvents which yield a simple site structure. The power of these methods is demonstrated by their ability to determine the frequency and intensity of the contribution to the band from the presence of the 1.1% of ^{13}C in the anion even though no separate resolved isotopic band is seen. The nature and origin of the characteristics of the anion site are considered in terms of the anion-solvent interaction. The features of both the cation-solvent and anion-solvent interaction which lead to the observed ion environment are treated. From these considerations, one may arrive at some physical properties which a solvent should have to bring about the kind of ion environment found in these six solvents. The role of the ion site found here in determining the chemistry of the $\text{Co}(\text{CO})_4^-$ anion in solution is illustrated with an example.

Experimental Section

Chemicals. The reagent grade tetrahydrofuran (THF) used in the preparation of the $\text{NaCo}(\text{CO})_4$ was a Baker "Analyzed Reagent." The dimethyl sulfoxide (DMSO) was obtained from J. T. Baker, the nitromethane and *N,N*-dimethylformamide (DMF) from Matheson Coleman and Bell, the acetonitrile and pyridine from Mallinckrodt, and the hexamethylphosphoric triamide from Eastman Organic Chemicals. The $\text{Co}_2(\text{CO})_8$ and CaH_2 were from Alfa Inorganics, the Na/K alloy (78% K; 99.95% pure) from M. S. A. Research Corp., and the molecular sieves (4 Å, pellets) from Union Carbide-Linde Division.

The Preparation of $\text{NaCo}(\text{CO})_4$. The $\text{NaCo}(\text{CO})_4$ was prepared by the reaction of $\text{Co}_2(\text{CO})_8$ and NaOH in THF.¹² The preparation was carried out in the apparatus shown in Figure 1. Five grams of NaOH (Mallinckrodt analytical reagent) was powdered under nitrogen in a polyethylene bag and placed in a weighed, stoppered vial. Two grams of $\text{Co}_2(\text{CO})_8$ was similarly placed in a weighed vial. The reaction apparatus was evacuated on a vacuum line and flamed to remove water. After cooling, it was filled with nitrogen on the vacuum line; the stopcocks were closed, and the apparatus was placed in the polyethylene bag with the vials of NaOH, $\text{Co}(\text{CO})_8$, a Teflon coated stirring bar, and a wide mouth funnel. The air in the bag was replaced with nitrogen and the apparatus opened, and NaOH and $\text{Co}_2(\text{CO})_8$ were placed in it as shown in Figure 1. (The use of the funnel in the NaOH addition prevents contact with the ground-glass joint.) The stirring bar is placed with the NaOH and the neck containing the $\text{Co}_2(\text{CO})_8$ is placed on the apparatus, sealing it. The reaction apparatus is

removed from the bag and connected to the vacuum line by attaching vacuum tubing to the two stopcocks.

About 15 ml of THF, purified as indicated below, is added through the serum stopple to the other arm of the vessel with a syringe which was dried in an oven at 140°. The stopcock below the serum stopple is closed and the apparatus tipped to pass the THF through the filter onto the NaOH. This process is speeded by placing a slight vacuum in the reaction side of the vessel *via* its stopcock to the vacuum line. Then the vessel is restored to an upright position and stirring is begun with an external magnetic motor. Then a partial vacuum is created in the vessel, the stopcock to the vacuum line closed, and the slow addition of the $\text{Co}_2(\text{CO})_8$ to the THF-NaOH mixture is begun. Gas evolution begins at this point and lasts for about 5 min.

The dark purple color of the $\text{Co}_2(\text{CO})_8$ disappears after about 0.5 hr but the stirring is continued for another hour. A light purple precipitate settles to the bottom along with unreacted NaOH within a few minutes after the stirring is stopped. The vessel is tipped and the cloudy yellow solution is filtered with vacuum through the fine glass frit to yield a pale yellow solution.

The THF is removed from the solution to a liquid nitrogen trap on the vacuum line by opening the vessel to the pump. To ensure removal of THF from the white powder which results, vacuum pumping is continued for 5 hr after the removal of the last liquid. Then the apparatus is filled with nitrogen on the vacuum line, closed, and removed to a polyethylene bag where the product is transferred under nitrogen to storage tubes.

The Purity of $\text{NaCo}(\text{CO})_4$. Water and THF are expected to be the primary contaminants of the salt and trace determinations were made for each. Water in the salt was detected by analyzing for it in a solution of the salt prepared from a dry solvent. A 0.01 M solution of the product in THF was made using dried solvent whose water content was established by an infrared method (see below) to be below 10^{-4} M. The solution is subjected to the same test for water. No additional water was found. Since it has been estimated that the lower limit of water detection by this method is 3×10^{-5} mol of water/l. of THF,¹³ the salt prepared as above can be considered dry for our purposes.

The $\text{NaCo}(\text{CO})_4$ prepared in this way was proved free of THF by examining the infrared spectrum of a Fluorolube mull of the salt (0.5 mol of $\text{NaCo}(\text{CO})_4$ per 100 g of Fluorolube) in the CH stretching region. No absorption due to the salt was detected. An upper limit of 6×10^{-4} mol of THF per mol of $\text{NaCo}(\text{CO})_4$ was established by examining the spectrum of Fluorolube containing weighed amounts of THF under the same conditions.

Solvent Preparation. The solvents used in this study were all degassed on a vacuum line to remove dissolved oxygen and dried by two or more exposures to molecular sieves. The following procedure employed with THF is typical of those used for the other solvents.

A Pyrex tube was filled three-fourths full with 300 ml of tetrahydrofuran and placed on a vacuum line. One hundred grams of molecular sieves was placed in a 500-ml round bottom flask which was closed by a stopcock *via* a connection. The flask was attached to the vacuum line *via* the stopcock, pumped briefly to remove the initial air, and then isolated from the line with the stopcock. The stopcock on the THF tube was opened to the line and the THF was alternately frozen with liquid N_2 and thawed while open to the pump. This process was repeated until the solvent was thoroughly degassed as indicated by the absence of bubbles of air rising to the surface of the liquid. After closing the stopcock to the THF, the molecular sieves were activated by heating to at least 300° for 30 min while keeping the flask open to the pump. After the sieves were cooled on the vacuum line (about 2 hr), they were isolated and the first 50 ml of THF was distilled into a liquid N_2 trap. Then 200 ml of THF was distilled onto the cooled sieves by placing an ice-water bath around the sieve flask.

The last 50 ml of THF remained behind in the tube. The THF was allowed to remain in contact with the sieves for 48 hr on the vacuum line while closed to the pump. The THF was then transferred onto another batch of freshly activated sieves in the same manner described above. The flask with the THF and sieves was then filled with N_2 on the vacuum line, removed from the vacuum line (stopcock closed), and allowed to stand for a few days before use. This flask was fitted with a serum stopple above the stopcock for later removal of the solvent.

(12) W. F. Edgell and J. Lyford, IV, *Inorg. Chem.*, **9**, 1932 (1970).

(13) W. F. Edgell and A. Barbetta, *Anal. Chem.*, submitted for publication.

In a typical example, after standing for 7 days, a sample of the THF was removed for a water determination, following the procedures outlined below. It showed 4×10^{-5} mol of water/l. of THF.

The same procedure was used to dry the six solvents used in the solution site studies, except that it was necessary to heat the DMF, HMPA, and DMSO to 50° in the distilling steps. To reduce the water in the solvents below 10^{-4} mol of water/l. of solvent, it was necessary to expose the solvents to fresh sieves the following number of times at the ratio of 50 g of sieves per 100 ml of solvent: THF (two times), pyridine (two times), DMSO (three times), CH_3NO_2 (four times), DMF (three times), HMPA (three times), and CH_3CN (three times).

Water Determination. The residual traces of water in each sieve-dried solvent was determined by an infrared spectrophotometric method. The details of the method are found elsewhere.¹³ The sensitivity is obtained by using the water fundamental at 2.8μ . The effects of solvent absorption at this wavelength is combated by ordinate scale expansion. The key to the method is the obtaining of the spectrum of a water-free sample of the solvent. These were prepared from sieve-dried solvents by removing the residual water from the sample after it was placed in the infrared cell. This was accomplished for THF and pyridine with Na/K alloy and for DMSO, DMF, HMPA, CH_3NO_2 , and CH_3CN with CaH_2 .¹³

Solution Preparation. The solutions studied were prepared by weighing a sample of $\text{NaCo}(\text{CO})_4$ in a 5-ml volumetric flask fitted with a serum stopple. All transfers were made under nitrogen in a polyethylene bag. First the flask and stopple were heated in an oven for several hours at 120° and then transferred to a nitrogen-filled polyethylene bag while still hot. The storage tube containing the $\text{NaCo}(\text{CO})_4$ was also placed in the bag and several exchanges of the atmosphere in the bag were accomplished with a roughing pump and a tank of nitrogen.

After the flask had cooled and was flushed with nitrogen, the stopple was placed in its opening. The flask was removed from the bag, weighed, transferred back to the bag, and the nitrogen atmosphere was restored.

The tube of $\text{NaCo}(\text{CO})_4$ was opened and a small amount was placed in the flask. The stopple was then replaced and the storage tube resealed. The flask was reweighed and returned to the bag.

A flask of solvent (outside the bag) was prepared for the transfer of liquid by placing a ground-glass socket on its ball joint about the stopcock. The socket was fitted with a serum stopple and the area between the stopcock and the stopple flushed with nitrogen admitted by a needle. The nitrogen was vented by use of a long, double ended needle that had been dried in the oven before being placed in the serum stopple. This process was continued for about 0.5 hr to remove all oxygen from the area above the stopcock. One end of the needle was forced through the polyethylene bag. The solvent flask stopcock opened and the other end of the needle was lowered into the solvent. A slight positive pressure was placed on the solvent to force a small amount of the liquid through the needle to wash it, the discharge emptying into a waste beaker in the bag. The end of the needle in the bag was then forced through the stopple on the volumetric flask, a small needle was placed through the stopple to vent nitrogen, and the volumetric flask was slowly filled with solvent to the mark. The solutions prepared in this way were 0.010 M in the salt.

The Infrared Spectra. The infrared spectra of the solutions were obtained between 1800 and 2030 cm^{-1} with a Perkin-Elmer 421 spectrometer. The grating change was set at 2080 cm^{-1} on this instrument to keep it well outside the region of interest under the conditions of operation. The spectral slit varied from 1.4 cm^{-1} at 1800 cm^{-1} to 1.7 cm^{-1} at 1950 cm^{-1} . An expanded wave number scale of $1 \text{ cm}^{-1}/2 \text{ mm}$ was used with a scan rate of $18 \text{ cm}^{-1}/\text{min}$. The gain and response was set to produce an active pen with a noise level of 0.25% T.

Standard Barnes Engineering cells with CaF_2 windows were used for the solutions. The thickness of the cell used for the HMPA solutions was found by the standard interference method to be 0.053 mm while that of the cell used for all other solutions was found to be 0.096 mm. A Perkin-Elmer variable-path cell with CaF_2 windows was filled with solvent and used in the reference beam of the spectrometer.

Filling the Cells, Running Spectra. The infrared cells were pumped in a vacuum desiccator for 12 hr. The desiccator was filled with nitrogen on the vacuum line immediately before a run and transferred to the polyethylene bag together with the volumetric flask containing the solution. A flask of solvent outside the bag was prepared for liquid transfer as described above in the section on sample preparation. After the nitrogen atmosphere is

established in the bag, the cells are removed from the desiccator and flushed with solvent obtained from the flask outside the bag *via* the doubled ended needle. Both the sample cell and the variable-path cell are filled with the solvent, the plugs forced in tightly, and the cells removed to the spectrometer where the variable-path cell is placed in the reference beam and the sample cell in the sample beam. The path length of the variable-path cell is adjusted to produce cancellation of the weak absorption bands of the solvent. The solvent base line is then established by scanning the region from 2080 to 1800 cm^{-1} .

After the base line is run, the sample cell is returned to the bag along with an oven-dried 1 ml syringe and needle still hot, and the nitrogen atmosphere is reestablished. Nitrogen is used to remove the solvent from the cell which is then washed several times by solution transferred from its flask with the syringe. (Be sure the syringe is completely cool.) The cell is filled with solution, the plugs placed tightly in position, and the cell removed to the spectrometer where the solution spectrum is run against the solvent in the variable-path cell.

Results and Discussion

In an electrolytic solution where the alkali ion frequency is independent of the identity of the anion, the dominant ion sites are solvent separated ion pairs and/or "free" ions.^{9a} The alkali ion bands from such solutions are broad and, because they lie in the far infrared where instrumentation problems abound, are not as well defined as bands which occur in the mid-infrared region. As a consequence, it is possible for a modest amount of a cation site which generates a spectral component which is anion dependent to be unnoticed. The detection of ions at such sites is desirable since they could be factors in some chemical reactions. When the alkali ion band shifts with change of the anion, contact ion pairs are present in the solution.⁸ The situation is the same as in the first case, for now a modest spectral component which does *not* vary with anion can lie undetected in the broad band nor can one see as separate components the spectral contributions from two sites whose cation frequencies are but a few wave numbers apart. Thus, the structural information obtained while accurate may be incomplete.

The C-O stretching vibrations of the $\text{Co}(\text{CO})_4^-$ have been shown to be a sensitive probe of solution structure at ion sites.¹¹ By observing them, it was possible to see both solvent separated ion pairs and contact ion pairs for $\text{NaCo}(\text{CO})_4$ in THF. These studies proceeded from the fact that an infrared (or Raman) band arising from an intramolecular vibration of an ion in solution is the sum of spectral contributions from the vibration of the ion in the various configurations which it occupies in the solution. The results already reported show two salient features. First, the solution structure could be understood in terms of distinct ion sites (not a continuum of sites). And second, the spectrum of the $\text{Co}(\text{CO})_4^-$ in different ion sites is sufficiently different that these components have a reasonable chance of being resolved in the complex band.¹¹

In the earlier work,¹¹ this resolution was made with an analog computer.¹⁴ It was used in a supporting role to measure the components of a complex band which were already revealed by the band changes brought about by variation of temperature and by the addition of water to the solution. As the present work proceeded, however, the role of the computer changed. First, it was found that a digital computer was required to express accurately all parts of the contour of

(14) The DuPont curve resolver.

a *single* infrared band. When such a computer was applied to this work, an immediate improvement was seen in the ability to describe the spectral bands. However, it was also found that this ability put a strain on the spectral data. One could use the computer to define a band with greater accuracy than it was defined experimentally by the chemical and spectroscopic methods. This situation led to the development of improved experimental methods.

The details of the experimental methods are presented in the Experimental Section above. On the spectroscopic side, it was necessary to expand the wave number scale of the recorded spectrum so that the band contour might be expressed with accuracy. Then slit widths must be as wide as possible to provide ample energy to enable the pen servo system to accurately track the changing spectrum. An upper limit to slit widths is fixed by the point at which band distortion results from the finite wave number interval of the radiation passing through the slits. Potts and Smith¹⁵ have shown that negligible distortion occurs when the slit width is one-fifth or less of the width of the band at half its maximum absorbance. Since the narrowest band studied in this work has a half-width of 17 cm⁻¹ (NaCo(CO)₄ in HMPA) and a maximum spectral slit of 1.7 cm⁻¹ was used to record the spectra, this criterion was safely met. As a further check on this point, the distortion introduced into the band envelope by the slit setting was calculated using a computer program written by Jones.¹⁶ It was found to be negligible, in agreement with the Potts-Smith criterion. The gain is set to produce a responsive pen and the inertia in the servo system set to reduce the noise to a level consistent with the accurate definition of the contour.

The spectra obtained in this way were reproducible. This was demonstrated by making a second run shortly after completion of the first. The two curves did not differ by more than the noise in all cases. Further elimination of the noise was obtained by averaging the two curves.

One additional point deserves attention before leaving the spectroscopic methods. Errors in the computer analysis of a band contour are sensitive to errors in the wave number scale produced by the spectrometer. This scale is readily corrected for a gradual, monotonic drift from "true wave number" by calibration with standard reference lines. On the other hand, a short-range excursion from "true wave number" is especially insidious in this work because it distorts the band in such a way to make it appear that an overlapped band is present where in fact none occurs. The spectrometer used in this work makes errors of this kind. They were detected and corrected by recording the interference fringes from an empty Irtran-2 cell with a path length of 0.5 mm. Fringe maxima and minima occur at equal spacing on a "true wave number" scale. Their deviation from this pattern on the spectrometer scale is a measure of the wave number error. The corrected wave number, ν_c , at any point in the range of the fringes was calculated by the equation

$$\nu_c = \nu_0 - (n + a/b)s$$

(15) W. J. Potts, Jr., and A. Lee Smith, *Appl. Opt.*, 6, 257 (1967).

(16) R. N. Jones, T. E. Bach, H. Fuhrer, V. B. Kartha, J. Pitha, K. S. Seshadri, R. Venkataraghavan, and R. P. Young, National Research Council of Canada Bulletin, No. 11, 1968.

where ν_0 is the true wave number of the reference maximum or minimum as determined by calibration with DCI gas, n is the number of maxima and minima between the reference maximum or minimum and the point of interest, a is the scale wave number distance of the point from the last maximum or minimum, and b is the scale wave number spacing between the maximum and minimum which spans the point. The correct spacing between maxima and minima, s , was determined by calibrating a maximum or minimum at the low wave number end of the fringe pattern with DCI or water vapor and counting fringes between the high wave number and low wave number calibration points. The validity of this calibration procedure was checked by using it to determine the wave numbers of lines in the DBr spectrum. No corrected value obtained by the above equation for any line differed by more than 0.3 cm⁻¹ from its accepted value. Thus, the wave number scale established by this fringe method may be taken as accurate to this extent. But most important, it is corrected for the wave number "surges" of the instrument.

Not only is it necessary that the spectrometer faithfully reproduce the spectrum of the sample but the sample must also be pure. Water is a solution contaminant which must be rigorously excluded. It has a strong affinity for the Na⁺ and a lesser one for the Co(CO)₄⁻. As a consequence, solutions which are so contaminated give a spectrum of the salt with water molecules as neighbors instead of the solvent molecules. To ensure that the spectra are those of the salt surrounded by solvent, the measurements were made on solutions which contained no more than one molecule of water per 100 molecules of salt. Since the salt concentration used was 10⁻² M, the water present must be less than 10⁻⁴ M. Unfortunately, the solvents used in this study have an affinity for water. Nevertheless, it is possible to dry them to the level set for this work, to prepare dry solutions, and keep them dry through the necessary operations. The procedures which evolved for this are given in the Experimental Section. The key to the elimination of the water contamination is a rapid, reliable method for its determination at this low level. The infrared method developed for this purpose is reported elsewhere.¹³

NaCo(CO)₄ was prepared by the reaction reported earlier.¹² The improved procedures used in this work are given above. The absence of water and THF in the product was demonstrated by analysis. The salt is a powerful reducing agent and reacts rapidly with O₂. Consequently, all operations with it are carried out under conditions in which air is rigorously removed and kept from the solvents and the solutions.

The spectra were run as indicated in the Experimental Section. The solvent base line, produced by running the solvent in the sample cell (sample beam) *vs.* the solvent in the variable-path cell (reference beam), was flat throughout the region. The solution curve, produced by running the solution in the sample cell *vs.* the solvent in the variable-path cell, coincided with the solvent base line outside the region of solute absorption. The per cent transmission for both the solution curve and the solvent base line was read from the instrument chart at equal spacing on the spectrometer wave number scale. The net absorbance of the dis-

solved $\text{NaCo}(\text{CO})_4$ was calculated at each wave number by the equation

$$A = \log (T_0/T)$$

where T is the transmission of the solution and T_0 of the solvent base line. The results for the salt in the six solvents are plotted against the corrected wave numbers in Figure 2.

A study of the Raman and infrared spectra of $\text{NaCo}(\text{CO})_4$ in solution from 3000 to 270 cm^{-1} shows that the $\text{Co}(\text{CO})_4^-$ ion is tetrahedral.¹⁷ This is confirmed by a recent X-ray study of the structure of crystalline $\text{TlCo}(\text{CO})_4$.¹⁸ An isolated ion of this structure would show one triply degenerate F_2 C-O stretching frequency in its infrared spectrum. This can be expected in solution near 1890 cm^{-1} .¹⁷ The actual details of the infrared spectrum in this region depends on how each specific $\text{Co}(\text{CO})_4^-$ interacts with its environment in the solution. If the effective forces at an anion are tetrahedral, one band would appear. On the other hand, if the effective forces are asymmetric, the three-fold degeneracy would be lifted and more than one band would occur in this spectral region. The observed band is the sum of components produced by each ion in the solution. The initial studies of solution spectra of this salt show that *both* situations can occur at ion sites, depending upon the solvent.^{8,11}

The infrared spectrum of $\text{NaCo}(\text{CO})_4$ in dimethyl sulfoxide, nitromethane, dimethylformamide, pyridine, hexamethylphosphoramide, and acetonitrile all apparently consist of one absorption band. A closer look at the band contours, especially by quantitative methods, raises some question on this point. It is the task of the band analysis to resolve this question. Such an analysis starts with a consideration of the shape expected for infrared bands. In a comprehensive review of this matter, Seshadri and Jones have concluded that the shape of a band from a substance in solution closely approximates a Lorentz (Cauchy) function when there is no solute-solvent interaction.¹⁹ Molecular interactions are expected to introduce a Gauss component into the band contour. Recent work of David and Hallam show that the absorption band shapes for SOCl_2 and SO_2 change with solvent.²⁰ Thus, the shape of one band of SOCl_2 dissolved in the nonpolar solvents CCl_4 , C_6H_4 , CS_2 , and *n*-hexane could be described by as Lorentz function to a "good approximation." The same absorption in CH_2I_2 and CHBr_3 solutions is "reasonably" well described by a Gauss function, while it shows a character intermediate between Gauss and Lorentz forms when Br_2 is the solvent. In view of these results, it is reasonable then to describe a band profile by a function which can reduce to either a Lorentz curve or a Gauss curve in the extremes and be a variable mixture of the two otherwise. Such a function can be formed as a product of the Lorentz and Gauss contributions or as a sum of them. Many attempts were made to fit the bands observed in this work with Gauss-Lorentz product functions. The results were poor, with the wing areas providing the

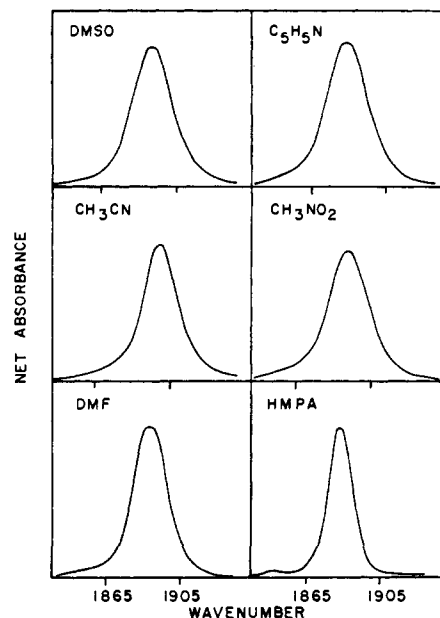


Figure 2. The infrared spectra of the CO stretching band for $\text{NaCo}(\text{CO})_4$ in several solvents.

major difficulty. On the other hand, it was possible to describe the profiles successfully with Gauss-Lorentz sum functions. For the general case where the experimental absorption band is made up of several overlapping bands, each one of which is described by a Gauss-Lorentz sum, the calculated absorbance at ν takes the form

$$A = \alpha + \sum_i \left\{ H_i / (1 + D_i^2(\nu - \nu_i^0)^2) + h_i \exp(-d_i^2(\nu - \nu_i^0)^2) \right\}$$

Here ν_i^0 is the center of the i th band in the absorption complex, H_i and h_i are the peak heights of the Lorentz and Gauss contributions to it, while D_i and d_i describe their half-widths through the relations

$$D_i = 1/LHW_i$$

$$d_i = \sqrt{\ln 2}/GHW_i$$

LHW_i is half the width of the Lorentz contribution to the i th band at half its peak absorbance while GHW_i is the corresponding quantity for the Gauss contribution. The sum is over the overlapping bands of the absorbance complex and the quantity α is added to take care of small shifts in the base line if needed.

To analyze a complex absorption band with this function, five parameters (ν^0 , H , h , D , and d) are to be fixed for each band in the complex. The computer program written for this purpose is very similar to one developed by Pitha and Jones.²¹ It uses a non-linear iterative procedure to minimize the difference between the experimental and the computer band profile. The quantity actually minimized is

$$\phi = \sum_n W_n^2 (AX_n - AC_n)^2$$

where AX_n is the experimental absorbance at the n th wave number point, AC_n is the calculated absorbance there, and W_n is a weighting number which expresses the

(21) J. Pitha and R. N. Jones, National Research Council of Canada Bulletin No. 12 (1968), and references cited therein.

(17) W. F. Edgell and J. Lyford, IV, *J. Chem. Phys.*, **52**, 4329 (1970).
 (18) D. P. Schussler, W. R. Robinson, and W. F. Edgell, *Inorg. Chem.*, in press.
 (19) K. S. Seshadri and R. N. Jones, *Spectrochim. Acta*, **19**, 1013 (1963).
 (20) J. G. David and H. E. Hallam, *J. Mol. Struct.*, **5**, 31 (1970).

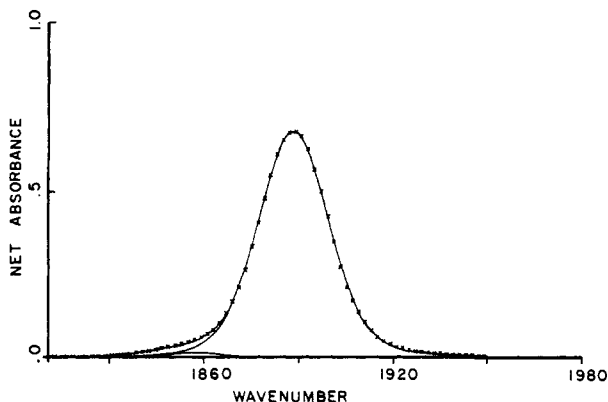


Figure 3. The resolution of the band for $\text{NaCo}(\text{CO})_4$ in DMSO: ($\times\times\times\times$) experimental, (—) computed.

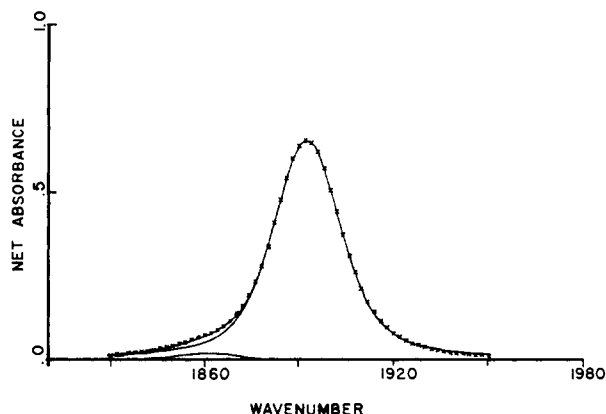


Figure 5. The resolution of the band for $\text{NaCo}(\text{CO})_4$ in CH_3NO_2 : ($\times\times\times\times$) experimental, (—) computed.

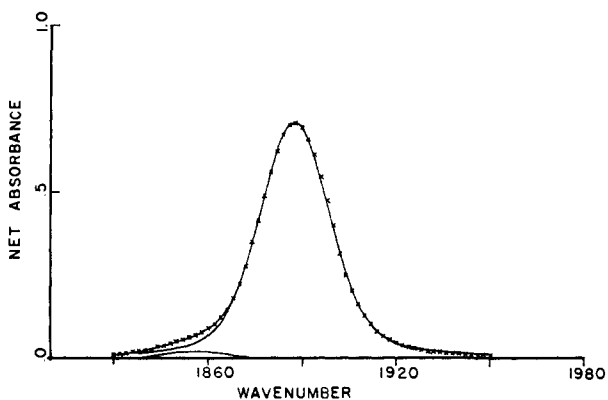


Figure 4. The resolution of the band for $\text{NaCo}(\text{CO})_4$ in pyridine: ($\times\times\times\times$) experimental, (—) computed.

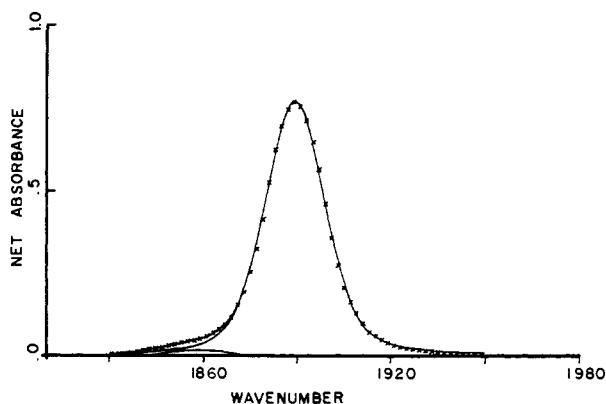


Figure 6. The resolution of the band for $\text{NaCo}(\text{CO})_4$ in DMF: ($\times\times\times\times$) experimental, (—) computed.

relative importance of a deviation at this point. The computations were made with a Control Data Corporation 6500 computer.

The absorption data obtained in this work include information far into the wings of each band. These long wings were a problem in the computer analysis since the points in the wings were sometimes greater in number than those in the central region where the absorbance is large. When the program was used with equal weights for all points, it would sacrifice agreement in the central region to better fit the band wings. Indeed, the weighting numbers were introduced to overcome this problem by giving more weight to the central region. The weight numbers used in this work gave the central region about a tenfold increase in weight over the wings. This produces small but tolerable errors in the wings while doing a better job in the central region.

The first solutions studied had DMSO and pyridine as solvents. When their data were analyzed by the computer, it became apparent that some small absorption near 1850 cm^{-1} existed in both bands that could not be accounted for by attributing all absorption to a single band. The existence of the second, very weak band proposed by the analysis became clearer to the unassisted eye with the study of the salt in DMF and then, especially, in hexamethylphosphoramide. When each of the six experimental bands were analyzed as a two-band system, the computer program was able to select two bands whose sum is in excellent agreement with the experimental contour. The results of this analysis are

shown in Figures 3 to 8 where the computed curves are compared with points taken from the experimental band. The frequency, integrated absorbance, and bandwidth at half-height for both bands in each solvent are collected in Table I.

Table I. Component Properties from Band Analysis^a

Solvent	ν_M	B_M	HW_M	ν_s	B_s
DMSO	1888.3	20.35	29.2	1854.9	0.37
CH_3NO_2	1892.5	21.18	25.8	1860.0	0.33
DMF	1889.3	20.47	22.0	1857.0	0.35
Pyridine	1887.7	22.12	27.0	1855.0	0.37
HMPA	1886.1	14.54 ^b	16.9	1851.0	0.22 ^b
CH_3CN	1892.8	18.70	21.3	1858.6	0.25

^a The units for all entries are cm^{-1} . ^b Converted to the same basis as the other solvents by multiplying the HMPA value by the ratio of the path length of the cell used with the other solvents to that used with HMPA (see Experimental Section).

The main component of these bands, ν_M , is assigned to the triply degenerate F_2 modes of the $\text{Co}(\text{CO})_4^-$ anion.

Turn now to the question of the origin of the side band. A band occurs near 1850 cm^{-1} for the $\text{Co}(\text{CO})_4^-$ ion in a contact ion-pair site for $\text{NaCo}(\text{CO})_4$ in THF¹¹ and such a site must be considered as a possibility for the origin of the side band. But the anion in the contact pair site also gives rise to a band at $\sim 1890\text{ cm}^{-1}$ which is roughly twice as intense as the

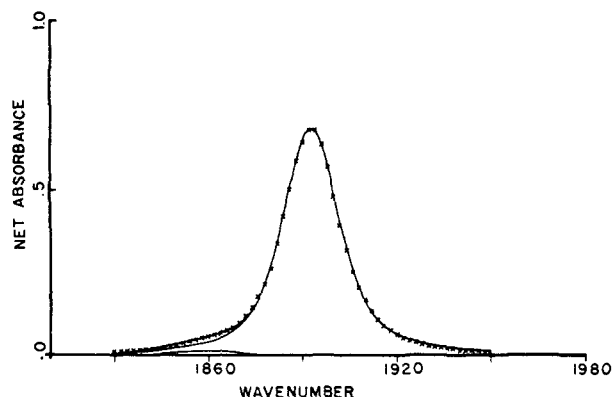


Figure 7. The resolution of the band for $\text{NaCo}(\text{CO})_4$ in CH_3CN : ($\times\times\times\times$) experimental, (—) computed.

1850- cm^{-1} band.¹¹ There is no indication of such a band in the six band contours of this study. Since such a band could be readily detected by the computer analysis in these systems if it existed, one must conclude that the side band has another origin.

Carbon-13 has a natural abundance of 1.1% so that 4.4% of the anions contain one isotopic atom. To compute the effect of the isotopic atom on a spectrum, we use first-order perturbation theory. In which case, the displacements of the atoms in each of the C-O stretching modes will show tetrahedral (T_d) symmetry as well as trigonal (C_{3v}) symmetry. Thus, there will be one C-O mode which will show the A_1 symmetry of C_{3v} and the F_2 symmetry of T_d . We designate this mode by the symbol A_1/F_2 . And there will be a pair of modes which show the E symmetry of C_{3v} as well as the F_2 symmetry of T_d designated here by E/F_2 . Thus, the isotopic anion will give rise to two frequencies

$$\Gamma = A_1/F_2 + E/F_2$$

in place of the single F_2 frequency shown by the normal anion. Theory shows that the E/F_2 frequency of the isotopic anion will be the same as the F_2 frequency of the normal anion. To calculate the A_1/F_2 frequency, we first computed force constants which reproduce the F_2 frequencies of the normal T_d anion.¹⁷ The distortion of the isotopic CO group is three times as large as that which occurs in each of the nonisotopic CO groups in the A_1/F_2 mode of the isotopic anion. Its frequency is directly computable from this fact plus the force constants and displacements from the T_d calculation. The results are that the A_1/F_2 frequency lies 34 cm^{-1} below the F_2 frequency of the normal anion.

The intensity of the A_1/F_2 band component may be computed as:

$$\frac{(1)(0.044)}{3(0.956) + (2)(0.044)} \times 100 = 1.5\%$$

of the intensity of the band component at the F_2 frequency. Note that the F_2 band component contains absorption from both the F_2 modes of the normal anion and the E/F_2 modes of the isotopic anion.

These calculations show that one should expect a weak band component of isotopic origin to lie 34 cm^{-1} below the intense band component of the normal anion and that its intensity would be 1.5% of that of the intense band component. The results of the band analysis in Table I show the side component to lie 33.4,

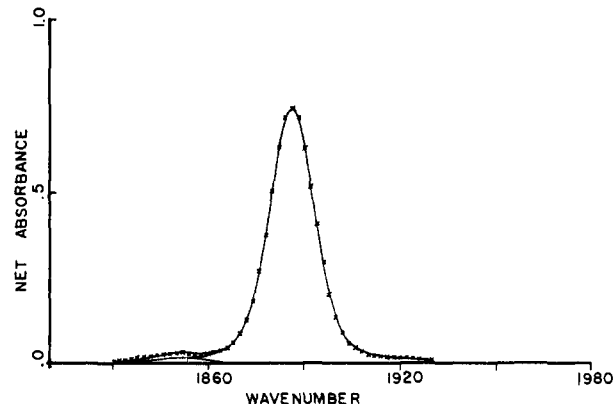


Figure 8. The resolution of the band for $\text{NaCo}(\text{CO})_4$ in HMPS: ($\times\times\times\times$) experimental, (—) computed.

32.5, 32.3, 32.7, 35.1, and 34.2 cm^{-1} below the main components in the six solvents. The side component intensities in Table I are 1.8, 1.6, 1.7, 1.7, 1.5, and 1.3% of the main component intensities for the six solvent systems. There can be no doubt about assigning the side component to the A_1/F_2 mode of the $\text{Co}(\text{CO})_3\text{C}^*\text{O}^-$ anion.

Besides the knowledge of the origin of the side band component, there are two additional points of some importance to be made from the above comparison of theory and experiment. Note that both the frequency and intensity of the side components were obtained from a computer-aided analysis of the experimental band contours. The first point is that the excellent agreement between the band properties and the expectations of theory demonstrates that this type of analysis can find ion sites of small population when the experimental data are accurate. And second, the inclusion of such sites will, in general, be required to obtain agreement between computed and experimental contours for data of high accuracy.

It is possible to make some comments about the solution structure at the ion sites. Within the limits of this experiment to detect differences, the site situation for the $\text{Co}(\text{CO})_4^-$ anion can be described by an effective potential energy for the vibration which has T_d symmetry. The vibration of the isotopic $\text{Co}(\text{CO})_3\text{C}^*\text{O}^-$ anions show C_{3v} symmetry. The comparison of theory and experiment above indicates that the reduction in symmetry at these sites can be understood as arising from the extra mass of the isotopic atom in an ion which is vibrating in an effective potential energy of T_d symmetry. Therefore, the solution environment of the anions consists of just one kind of ion site, a site with effective T_d symmetry in its vibrational potential energy. Can this symmetry in the effective potential energy arise from the averaging associated with a rapid rotation of the anion in its environment? This seems hardly likely. The moment of inertia for the anion of $\sim 815 \times 10^{-40} \text{ g cm}^2$ confines it to a ponderous rotary motion at room temperature which is matched by the rather ponderous rotation and translational motion of the solvent molecules (relative to the vibrational motion of the anion). Can the effective T_d symmetry mean that the anion feels no forces at all from its environment? If this was true, the anion would be freely rotating, albeit ponderously. Another unlikely situation. Does it mean that the solution geometry at an

anion actually shows T_d symmetry? Also not probable. What these experimental results probably mean is that the forces on the anion coming from its environment, while large enough to influence its rotary-translatory motion, are small relative to the forces required to distort the C-O bonds of the anion. The absorption experiment sums the interaction of the radiation field with all the anions of the solution. This average over all the anions is statistically equivalent to an average over the time behavior of a single anion. And in this average the effect of the solution environment on the anion is smoothed to the effective T_d character.

What the observed T_d character of the effective anion site potential energy means structurally is that the Na^+ ion is not a near neighbor of the anion in these solutions. This follows from the results for $\text{NaCo}(\text{CO})_4$ in THF which suggest that the presence of the Na^+ ion in the immediate environment of the anion produces a strong distortion of the T_d character of its effective potential energy.¹¹

Some qualitative comments can be made about the interaction of the anion with the solvent molecules. Table I shows that the frequency of the main bond is almost the same in all the solvents. The differences although small are real, however. A major portion of the anion-solvent interaction is expected to be the same in all these systems, since it is less important what neighbor occupies a given place than that some neighbor be there. The frequency differences in Table I reflect only differences in the unique part of this interaction.

The integrated absorption coefficient is another measure of the anion-solvent interaction. The absorption may be visualized classically as arising from the change in the electric dipole which results from the vibrational motion and its intensity is proportional to this dipole change. The dipole change may be thought of as having three components: the portion which results from the distortion of the anion charge distribution during the anion vibration in the absence of any neighbors, the change in the anion charge distribution during the vibration as a result of its distortion by the solvent neighbors (*e.g.*, electron cloud overlap effects), and the charge distortion of the solvent molecules which occurs during the anion vibration. The variation in these last two effects as one changes solvent is reflected in the variations in the integrated absorption coefficients found in Table I. The pronounced differences seen here indicate that the consequences of anion-solvent interaction on the dipole behavior at the ion site change markedly with solvent change.

The width of the main band at half its center intensity is another probe of anion-solvent interaction. The width depends upon the time development (*i.e.*, relaxation) of the *direction* of the vibrating dipole discussed above. The more rapidly this direction changes the broader the band. An examination of the half-widths in Table I shows significant differences with solvent in this spectral feature of the bands. These results show that the anion interacts in significant ways with the solvents of this study.

We turn now, to the question of what properties of these solvents result in the single kind of ion site in which the anion sees only solvent molecules in its near environment and has an effective site symmetry of T_d .

What one has to understand is why the Na^+ cation is not a near neighbor of the $\text{Co}(\text{CO})_4^-$ anion. This reduces to a consideration of two "drives" in the solution: that of the solvent molecule to get near the anion and that of the solvent molecule to get near the cation. For either or both of the drives to produce any results, they must be stronger than the forces which hold the solvent molecule in the liquid solvent structure. Or stated another way, the forces which one or both ions exert on a solvent molecule must be greater than the forces on the solvent molecule exerted by the other solvent molecules of the liquid. And this differential must be sufficiently great to alter the structure at one or both ions from that of the pure solvent. Of course, the electrical effects are not the whole explanation, for the molecular geometries must permit the structures to be established and the forces holding it together must prevail over the dispersive (entropic) effects of the thermal energy. With these caveats out of the way, we turn now to the electrical effects. The $\text{Co}(\text{CO})_4^-$ anion is large and its negative charge is dispersed. Consequently, the electrical force which it exerts on a charge in its near neighborhood is small. Thus, it has a weak aligning effect on the solvent molecule of this study for which the center of positive charge tends to be buried in the bulk of the molecule. In contrast, the Na^+ is small and the force (gradient of its electrical potential) it exerts on a charge nearby is relatively large. Moreover, all the solvents of this study have strong centers of negative charge. Thus, a dominant factor in determining ion site structure in these solutions is the tendency to form structure at the Na^+ ion. We have noted that strong centers of negative charge in the solvent molecules are a major factor in forming such structure. But the anion also has centers of negative charge which generate forces which push it toward the cation. And thus, the matter reduces to a competition between the solvent molecules and the anion for a place next to the Na^+ ion. The experimental results show that for all the solvents here, the forces between the solvent molecules and Na^+ are sufficiently large compared to those between the $\text{Co}(\text{CO})_4^-$ ion and the Na^+ ion so that (with the help of their greater numbers) they are able to exclude the $\text{Co}(\text{CO})_4^-$ anion from the near-neighbor shell of the Na^+ ion.

Thus, a solvent must have a high donor ability to form ion sites of the simple variety found in this study, but it makes a difference how the donor ability of the solvent is measured. Gutmann has devised a donor number scale based on the interaction of a solvent with SbCl_5 .²² This scale is successful in allowing one to understand a range of phenomena in coordination chemistry. Table II shows the donor numbers for the

Table II. The Donor Number of the Solvents

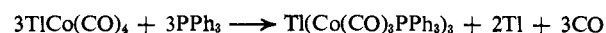
Solvent	Donor no. ²²	Solvent	Donor no. ²²
CH_3NO_2	2.7	DMSO	29.8
CH_3CN	14.1	Pyridine	33.1
DMF	26.6	HMPA	38.8

(22) V. Gutmann, "Coordination Chemistry in Non-Aqueous Solutions," Springer-Verlag, New York, N. Y., 1968, and references cited therein.

solvents of this study. It is seen that the solvents cover virtually the whole range of the donor numbers. All of the solvents, however, show a donor ability of sufficient strength to bring about the simple T_d ion site structure. Thus, the phenomena of ion site character is not included in the donor number as measured by solvent-SbCl₅ interaction.

The chemistry of a salt in solution is just the sum of the chemistry at the ion sites. What makes this statement nontrivial is an expectation that the chemistry will generally be different at the different ion sites. The nature of an ion site in solution can be expected to have a role in both the quantitative and qualitative aspects of reactions in which it is involved either directly as a reactant or indirectly as a catalyst. The qualitative importance of the solvent surrounded ion

site found for the $\text{Co}(\text{CO})_4^-$ ion in these solvents is demonstrated by the reaction



which, while it takes place in selected nonaqueous solvents, does *not* occur at solvent surrounded ion sites.^{17,23}

Acknowledgment. The authors wish to thank the National Science Foundation for its support of this work under Grant No. GP-27928 and under the Purdue NSF-MRL Program and Mr. Paul Luxix for his assistance in preparing the computer tracings from which Figures 3-8 were made. We thank the Minnesota Mining and Manufacturing Co. for a fellowship for A. B. during the 1971-1972 academic year.

(23) W. F. Edgell, W. R. Robinson, A. Barbetta, and D. P. Schussler, *J. Amer. Chem. Soc.*, in press.

Solution Thermodynamics in Nonideal Mixed Solvents under Endostatic Conditions¹

Ernest Grunwald* and Adan Effio

Contribution from the Chemistry Department, Brandeis University, Waltham, Massachusetts 02154. Received May 7, 1973

Abstract: Thermodynamic functions of solution, reaction, and activation measured in nonideal mixed solvents of constant composition are inherently complex because the addition of a solute under such conditions is attended by changes in the relative partial molal functions of the solvent components. This complexity is avoided if the thermodynamic functions are measured under endostatic conditions, that is, in such a way that the ratio a_1/a_2 of the activities of the solvent components remains constant. Precise definitions are given, and it is shown that functions measured under endostatic conditions in mixed solvents are exactly analogous to corresponding functions in one-component solvents. Thermodynamic equations are derived for transforming data obtained at constant composition to constant a_1/a_2 . Solvent properties required in such transformations are tabulated for common water-organic solvent mixtures. The use of endostatic functions is illustrated for the solvolysis of *tert*-butyl chloride in ethanol-water mixtures.

Equilibrium and rate constants and thermodynamic properties of solutes in binary liquid solvent systems are sometimes inordinately complex when studied as a function of temperature, pressure, solvent composition, or neutral-salt addition. This is particularly true for water-organic mixed solvents, and for those thermodynamic functions for which the solvent system itself shows marked deviations from ideal behavior.^{2,3} For example, in water-organic mixtures, activation energies, activation volumes, and heats of solution as a function of solvent composition often show maxima and/or minima;⁴⁻⁷ partial molal heat

capacities of solutes may show several inflections and differ greatly from molar heat capacities in the pure state;^{8,9} and neutral-salt effects may become specific for each salt so that they can no longer be treated as colligative functions of the ionic strength.^{10,11}

Unfortunately, the mixed solvents which display the greatest deviations from ideal thermodynamic behavior are precisely those of the greatest practical utility. This is because there is little advantage in using a mixed solvent (rather than a pure one) unless the solvating actions of the components are genuinely different and complementary. Thus, familiar patterns of behavior associated with solutions in one-component solvents and ideal mixtures often become distorted in common mixed solvents. For example, the hydrolysis of triethyl orthobenzoate almost certainly proceeds with specific hydrogen ion rather than general acid catalysis.¹¹ However, owing to the peculiarities of neutral kinetic

(1) This work was supported in part by a grant from the National Science Foundation.

(2) For a representative symposium, see "Hydrogen-Bonded Solvent Systems," A. K. Covington and P. Jones, Ed., Taylor and Francis, London, 1968.

(3) F. Franks and D. J. G. Ives, *Quart. Rev., Chem. Soc.*, **20**, 1 (1966).

(4) (a) A. H. Fainberg and S. Winstein, *J. Amer. Chem. Soc.*, **78**, 2770 (1956); (b) S. Winstein and A. H. Fainberg, *ibid.*, **79**, 5937 (1957).

(5) J. B. Hyne, R. Wills, and R. E. Wonkka, *J. Amer. Chem. Soc.*, **84**, 2914 (1962).

(6) (a) E. M. Arnett, W. G. Bentrude, J. J. Burke, and P. M. Duggleby, *J. Amer. Chem. Soc.*, **87**, 1541 (1965); (b) E. M. Arnett, W. G. Bentrude and P. M. Duggleby, *ibid.*, **87**, 2048 (1965).

(7) (a) J. B. Hyne, H. S. Golinkin, and W. G. Laidlaw, *J. Amer. Chem. Soc.*, **88**, 2104 (1966); (b) H. S. Golinkin, I. Lee, and J. B. Hyne, *ibid.*, **89**, 1307 (1967); (c) C. S. Davis and J. B. Hyne, *Can. J. Chem.*, **50**, 2270 (1972).

(8) (a) E. M. Arnett and D. R. McKelvey, *J. Amer. Chem. Soc.*, **87**, 1393 (1965); (b) E. M. Arnett and D. R. McKelvey, *ibid.*, **88**, 5031 (1966).

(9) R. E. Robertson and S. E. Sugamori, *J. Amer. Chem. Soc.*, **91**, 7254 (1969).

(10) (a) E. Grunwald and A. F. Butler, *J. Amer. Chem. Soc.*, **82**, 5647 (1960); (b) E. F. J. Duynstee, E. Grunwald, and M. L. Kaplan, *ibid.*, **82**, 5654 (1960).

(11) P. Salomaa, A. Kankaanperä, and M. Lahti, *J. Amer. Chem. Soc.*, **93**, 2084 (1971).